

Article

Linking Bacterial Rhizosphere Communities of Two Pioneer Species, *Brachystegia boehmii* and *B. spiciformis*, to the Ecological Processes of Miombo Woodlands

Camilo B. S. António ^{1,2}, Chinedu Obieze ^{3,4,†}, João Jacinto ^{5,†}, Ivete S. A. Maquia ^{2,6,†}, Tara Massad ⁷, José C. Ramalho ², Natasha S. Ribeiro ^{8,9}, Cristina Máguas ^{1,5}, Isabel Marques ^{2,*}
and Ana I. Ribeiro-Barros ^{1,2,*}

- ¹ BioEducation Consortium (Gorongosa National Park, Instituto Superior Politécnico de Manica, Universidade Lúrio, Universidade Zambeze, and Universidade de Lisboa), Gorongosa National Park, Gorongosa P.O. Box 1983, Mozambique
- ² Forest Research Center (CEF) & Associated Laboratory TERRA, School of Agriculture, University of Lisbon, 1349-017 Lisboa, Portugal
- ³ Africa Centre of Excellence in Oilfield Chemicals Research, University of Port Harcourt, Port Harcourt 500272, Rivers State, Nigeria
- ⁴ Centre D'étude de la Forêt, Institut de Biologie Intégrative et Des Systèmes, Université Laval, Quebec City, QC G1V 0A6, Canada
- ⁵ Ce3C—Centre for Ecology, Evolution and Environmental Changes, Faculdade de Ciências, Universidade de Lisboa, 1649-004 Lisboa, Portugal
- ⁶ Biotechnology Center, Eduardo Mondlane University, Maputo 3453, Mozambique
- ⁷ Department of Scientific Services, Gorongosa National Park, Gorongosa P.O. Box 1983, Mozambique
- ⁸ Department of Environmental Sciences, University of Virginia, Charlottesville, VA 22903, USA
- ⁹ Faculty of Agronomy and Forest Engineering, Eduardo Mondlane University, Maputo 3453, Mozambique
- * Correspondence: isabelmarques@isa.ulisboa.pt (I.M.); aribeiro@isa.ulisboa.pt (A.I.R.-B.)
- † These authors contributed equally to this work.



Citation: António, C.B.S.; Obieze, C.; Jacinto, J.; Maquia, I.S.A.; Massad, T.; Ramalho, J.C.; Ribeiro, N.S.; Máguas, C.; Marques, I.; Ribeiro-Barros, A.I. Linking Bacterial Rhizosphere Communities of Two Pioneer Species, *Brachystegia boehmii* and *B. spiciformis*, to the Ecological Processes of Miombo Woodlands. *Forests* **2022**, *13*, 1840. <https://doi.org/10.3390/f13111840>

Academic Editors: Hui Li and Yuguang Zhang

Received: 23 September 2022

Accepted: 1 November 2022

Published: 4 November 2022

Publisher's Note: MDPI stays neutral with regard to jurisdictional claims in published maps and institutional affiliations.



Copyright: © 2022 by the authors. Licensee MDPI, Basel, Switzerland. This article is an open access article distributed under the terms and conditions of the Creative Commons Attribution (CC BY) license (<https://creativecommons.org/licenses/by/4.0/>).

Abstract: Miombo is the most extensive ecosystem in southern Africa, being strongly driven by fire, climate, herbivory, and human activity. Soils are major regulating and supporting services, sequestering nearly 50% of the overall carbon and comprising a set of yet unexploited functions. In this study, we used next-generation Illumina sequencing to assess the patterns of bacterial soil diversity in two pioneer Miombo species, *Brachystegia boehmii* and *Brachystegia spiciformis*, along a fire gradient, in ferric lixisol and cambic arenosol soils. In total, 21 phyla, 51 classes, 98 orders, 193 families, and 520 genera were found, revealing a considerably high and multifunctional diversity with a strong potential for the production of bioactive compounds and nutrient mobilization. Four abundant genera characterized the core microbiome among plant species, type of soils, or fire regime: *Streptomyces*, *Gaiella*, *Chthoniobacter*, and *Bacillus*. Nevertheless, bacterial networks revealed a higher potential for mutualistic interactions and transmission of chemical signals among phylotypes from low fire frequency sites than those from high fire frequency sites. Ecological networks also revealed the negative effects of frequent fires on the complexity of microbial communities. Functional predictions revealed the core “house-keeping” metabolisms contributing to the high bacterial diversity found, suggesting its importance to the functionality of this ecosystem.

Keywords: *Brachystegia*; carbon; functional potential; legumes; metagenomics; rhizosphere; C and N stable isotopes

1. Introduction

The Miombo woodlands are the dominant type of vegetation in southern Africa, placed among the 35 priority ecoregions defined by the World Wide Fund Global Program Framework [1]. Miombo extends over ca. 2 million ha through seven countries: Angola, the Democratic Republic of the Congo, Malawi, Mozambique, Tanzania, Zambia, and

Zimbabwe [2]. These woodlands provide multiple ecosystem services of economic, social, and ecological relevance, such as timber, food, medicines, biomass, energy, water, and carbon balance [3,4].

Miombo is dominated by trees from the Fabaceae family (legumes), predominantly belonging to the genera *Brachystegia*, *Julbernardia*, and *Isoberlinia* [5]. The ecological dynamics of the woodlands are strongly influenced by fire, which results from a combination of natural and anthropogenic factors [6]. While fire is required to maintain the phytosociological structure of Miombo, high frequency fire regimes impose negative changes on the structure and composition of vegetation [7]. Understanding the interactions between fire and Miombo vegetation is thus necessary for the implementation of efficient resource conservation and management strategies.

Soils provide major regulating and supporting services in Miombo, sequestering nearly 50% of the overall carbon [8]. A recent study in one of the most extensive and pristine areas of Miombo, the Niassa Special Reserve (Mozambique), revealed that the bacterial community in Miombo soils is highly diverse, comprising a set of yet unexploited functions [9]. Soil microorganisms play crucial roles in biogeochemical cycles, nutrient and water transportation, plant health and performance, soil structure, and fertility [9,10]. Microorganisms can stimulate plant growth through the production of growth regulators like hormones, protect plants against pathogens through competition, solubilize phosphate, produce organic matter, or remediate polluted soils [11]. One gram of forest soil harbors millions to billions of bacteria that underlie soil dynamics and serve as indicators of ecosystem health and land-use [12]. Thus, in association with climate and anthropogenic factors, the soil microbiome is a major ecological determinant of ecosystem services [13]. However, despite the importance of soil microorganisms, they are understudied, particularly in Miombo, where soil microorganisms and plant-microbe interactions remain largely undescribed [9,14,15].

Biological nitrogen fixation (BNF) by mutualistic bacteria is just one example of the interactions that require in-depth study in Miombo, which is dominated by legume trees, generally known for fixing N_2 . BNF often constitutes the main entry pathway of N into ecosystems [16]. As N is often one of the most limiting elements in soils, symbiotic associations with N-fixing bacteria, like rhizobia, offer a competitive advantage to plants [17]. Thus, understanding BNF in nutrient-poor Miombo ecosystems is of utmost importance. The composition of stable nitrogen ($^{15}N/^{14}N$) and carbon ($^{13}C/^{12}C$) isotopes is a useful proxy to understand the environmental impact on ecophysiological processes associated with biogeochemical cycles as well as the interactions between the biosphere, pedosphere, and atmosphere [17]. In general, the natural abundance of ^{15}N provides information about the N sources used by plants and N fluxes in ecosystems. As N_2 -fixing species typically have $\delta^{15}N$ signatures close to atmospheric values, $\delta^{15}N$ is used as a tracer of N within an ecosystem [18]. C isotopes are also illustrative indicators of ecosystem dynamics and are used to measure plant performance at the photosynthetic level, reflecting an integrated value for water use efficiency [19].

The present study was undertaken to assess the changes in the soil microbiome of two characteristic Miombo species, *Brachystegia spiciformis* Benth. and *Brachystegia boehmii* Taub. (Fabaceae: Detarioideae), in response to soil type and fire regimes. As fires are becoming more frequent in this ecoregion [20], characterizing changes in the microbiome diversity, composition, and microbial functional potential helps to capture microbial dynamics that might be relevant to ecosystem recovery. This has been completed with stable C and N isotope analysis to further explore the functional dynamics of Miombo woodlands.

2. Materials and Methods

2.1. Site Description and Experimental Design

Fieldwork was conducted in Gorongosa National Park in Mozambique (GNP; Sofala Province, 18.766° S 34.5° E). The climate is Aw (equatorial savanna with dry winter) according to the Köppen–Geiger climate classification system [21]. Mean annual rainfall is

ca. 900 ± 300 mm and the average temperature is ca. 23 °C. Native Miombo vegetation is dominated by *Brachystegia spiciformis*, *Brachystegia boehmii*, and *Julbernardia globiflora*. Besides their ecological importance, these species have a relevant economic role for rural and urban communities as they are used for many purposes, including fabric cords, furniture, and bee hives [22]. Rhizosphere soils of *B. boehmii* and *B. spiciformis* were collected in 1 ha permanent plots, established in two areas with different soil types, i.e., ferric lixisol and cambic arenosol soils, and exposed to different fire regimes: high fire frequency (HFF) and low fire frequency (LFF) [23]. Ferric lixisols have clays with a low cation exchange capacity, while cambic arenosols are sandy-textured soils with little profile development [24]. A total of 24 samples were collected from rhizosphere soils, as well as the leaves of three individuals from each species (Table 1). Focal individuals had a minimum diameter at breast height (DBH) of 15 cm and were at least 10 m apart from the nearest neighboring tree. Soil samples were collected 10 cm from the base of each focal tree using the shake method, at a depth of 20–30 cm with a plated soil probe (401.01, AMS Inc., Harrison, AR, USA). Samples were placed in plastic bags and kept on ice for a maximum of 6 h and stored at -80 °C before DNA extraction. Mature, undamaged leaves from the same three individuals of each focal species were stored in labeled plastic bags, kept on ice for a maximum of 6 h, and then dried at 60 °C for 48 h. Dried samples were stored at 4 °C until they were processed for isotope analyses.

Table 1. Sampling information: soil type, fire frequency, and geographical coordinates.

Soil Type	Fire Frequency	Fire Interval	Latitude	Longitude
Cambic arenosol	High	1 year	-19.00125	34.20163
	High	1 year	-19.00135	34.20174
	Low	6 years	-19.00009	34.20236
	Low	6 years	-18.99999	34.20720
Ferric lixisol	High	1 year	-18.95165	34.17806
	High	1 year	-18.95198	34.17942
	Low	6 years	-18.96186	34.16772
	Low	6 years	-18.96351	34.16873

2.2. Genomic DNA Extraction, Library Construction, and Illumina Sequencing

Total genomic DNA was extracted from 100 mg of soil using the DNeasy PowerSoil Kit (Qiagen, Germantown, MD, USA) following the manufacturer’s instructions. To analyze the bacterial composition of the samples, the 16S rRNA genes of the V3-V4 regions were amplified by polymerase chain reaction (PCR) using the primers, V3/V4 341F (5'-CCT ACG GGG NGG CWG CAG-3') and 805R (5'-GAC TAC HVG GGT ATC TAA TCC-3') with barcodes at the 5' and 3' ends of the DNA fragments. The following conditions were used: initial denaturation at 98 °C for 2 min, followed by 35 cycles of denaturation at 95 °C for 30 s, primer annealing at 53 °C for 40 s, extension at 72 °C for 1 min, and a final extension phase at 72 °C for 5 min. Sequencing libraries were generated using a TruSeq DNA PCR-free sample preparation kit (Illumina, San Diego, CA, USA) following the manufacturer’s instructions. The final libraries were sequenced using the Illumina MiSeq platform to generate 300 bp paired-end reads through Macrogen sequencing services (Macrogen, Seoul, Korea).

2.3. Assembly of Reads and Taxonomical Assignment

Raw sequences were checked and trimmed using QIIME v.1.7.0 [25] to remove short and low-quality sequences that contained less than 200 bp, ambiguous bases, and those with a minimum quality score of 20. Clean paired-end reads were merged using FLASH v. 1.2.11 [26], a very fast and accurate analysis tool designed to merge paired-end reads when the original fragments are shorter than twice the length of the reads, resulting in longer reads that can significantly improve genome assemblies. Potential chimeric sequences were identified and removed by the UCHIME algorithm [27]. Unique sequences

were grouped in operational taxonomic units (OTUs) with 97% similarity using VSEARCH v.6.1.544 applying a 3% dissimilarity cut-off [28]. Pruning of OTUs with a low number of sequences (<5) was carried out on a per-sample basis, as an OTU that is common in one sample may occur as a low-abundance contaminant in others owing to cross-contamination. The most abundant sequence of each OTU was selected as representative. Taxonomy was assigned through a search for similar sequences conducted with BLAST v2.2.29 using a similarity coefficient of 98% against the Greengenes (version 13_5) online database [29]. This 16S rRNA gene database is a curated database that addresses the limitations of public repositories such as NCBI by providing chimera screening, standard alignment, and taxonomic classification using multiple published taxonomies.

QIIME v.1.9.1 was used to calculate the Shannon–Wiener (H') alpha diversity index with the package `alpha_diversity` [30]. The software was also used to produce rarefaction curves to compare the richness of different OTUs using the package `alpha_rarefaction.py`. The UniFrac distance between samples [31] was visualized using a principal coordinate analysis (PCoA). A *t*-test or an ANOVA was used to test the presence of significant differences in the number of OTUs, in the diversity index, and in the abundance of taxonomic groups using STATISTICA v.13.3 (TIBCO Software Inc. 2017, Palo Alto, CA, USA) between plant species, soil types, and fire frequency. In addition, a differential abundance analysis was performed to determine the most responsive phylotypes to frequent fire based on LefSe [32] and a random forest test [33].

The co-occurrence patterns of bacterial communities were investigated based on Pearson's correlation coefficient using Molecular Ecological Network Analysis Pipeline (MENAP; [34]). To increase statistical power and reduce the occurrence of spurious correlations, the networks were constructed using samples grouped according to HFF and LFF, regardless of differences in soil types. In addition, to reduce the complexity of the networks, only the bacterial genera occurring in at least 50% of the samples for each group were used for the construction of the network. Spurious indirect bacterial associations were removed using the iDIRECT algorithm implemented in MENAP. The constructed empirical networks were compared against their 100 corresponding random networks, following the Maslov–Sneppen procedure [35], as implemented in MENAP. To identify keystone species, network connectivity was determined by calculating the within the module (Z_i) and among the module (P_i) connectivity of each node. Based on this criterion, the network nodes were assigned as follows: (i) peripheral nodes ($Z_i \leq 2.5$, $P_i \leq 0.62$), (ii) connectors ($Z_i \leq 2.5$, $P_i > 0.62$), (iii) module hubs ($Z_i > 2.5$, $P_i \leq 0.62$), and (iv) network hubs ($Z_i > 2.5$, $P_i > 0.62$; [36]).

2.4. Functional Prediction of Miombo Soils

Functional profiles were predicted using the R package Tax4Fun v 0.3.1 [37] based on the OTU table produced by QIIME v.1.7.0 and visualized using MicrobiomeAnalyst [38]. Tax4Fun is a software package that predicts the functional capabilities of microbial communities based on 16S rRNA datasets [37]. In addition, functional predictions of the bacterial community were carried out by AllGenetics & Biology SL using the software PICRUSt2 [39]. Contrary to Tax4Fun, PICRUSt2 infers the microbial gene content of each OTU and predicts the abundance of the different gene families and metabolic pathways potentially present in the microbial community. We used the hidden state prediction tool, implemented in the `castor` R package [40], to normalize the data and predict gene family profiles. To generate a finer resolution of the predicted changes within the metagenomes, we weighted the results of the prediction of gene families by the relative abundance of the OTUs to infer the metagenomes of the community, using the BIOM tables with OTU abundances per sample. We mapped EC abundances onto gene pathways using MinPath [41] and the MetaCyc reactions database [42]. The resulting pathway abundance table represents how much each OTU contributes to the community-wide pathway abundance. We used the package STAMP [43] to perform the statistical analysis of the functional profiles recovered using the two-sided Welch's *t*-test. The Benjamini–Hochberg FDR [44] correction method was

applied to the results and all features with a $p \geq 0.05$ were removed. A scatter plot was generated to easily visualize the level of correlation between samples.

2.5. Isotopic Composition and Elemental Analysis

Oven-dried leaf samples were ground to a fine powder with a mill (MM2, Retsch, Haan, Germany), as described in [45]. For the isotopic ($\delta^{13}\text{C}$ and $\delta^{15}\text{N}$) and elemental analyses, 0.5 mg of each sample was weighed out into tin capsules. The analysis of stable isotopes was carried out on a continuous flow isotope ratio mass spectrometer (CF-IRMS, Haan) on a Sercon Hydra 20–22 (Hydra 20–22, Sercon, Crewe, UK) coupled to a EuroEA elemental analyzer (EuroVector, Pavia, Italy) for online sample preparation by Dumas-combustion. Isotopic ratios for carbon and nitrogen were calculated using the standard δ notation:

$$\delta X = \left(\left(\frac{R_{\text{sample}}}{R_{\text{reference}}} \right) - 1 \right) * 1000 (\text{‰})$$

where $X = \text{C}$ or N and $R = \delta^{13}\text{C}/\delta^{12}\text{C}$ for C and $\delta^{15}\text{N}/\delta^{14}\text{N}$ for N [46]. The reference for $\delta^{15}\text{N}$ was air and PeeDee Belemnite (PDB) for $\delta^{13}\text{C}$. Reference materials used were USGS-25, USGS-35, BCR-657, and IAEA-CH7 [47]. The standard used was wheat flour standard OAS (Elemental Microanalysis) for both N and C . Precision of the isotope ratio analysis was calculated using 6–9 replicates of laboratory standard material interspersed among samples in every batch analysis and was $\leq 0.1\%$. The main mass signals of N and C were used to calculate the total abundances of N and C using OAS with 1.47% C and 39.53% N as a reference for elemental composition. Changes in $\delta^{13}\text{C}$, $\delta^{15}\text{N}$, C , N , and C/N as a result of fire frequency, soil type, and species were analyzed with a two-way ANOVA.

3. Results

3.1. Microbial Community Composition and Diversity

Sequencing recovered a total of 96,144,192 bp from 211,854 reads with an average G/C ratio of 57.32% (Supplementary Table S1). After the removal of low-quality sequences and chimeras, 97.46% of the reads passed the Q20 filter and 90.80% passed the Q30 filter. Owing to the high depth of sequencing, the rarefaction curves (Supplementary Figure S1) showed a high coverage approaching saturation in all of the samples.

The rhizosphere of the two plant species shared a similar number of OTUs. An average of 1048 ± 107 OTUs were identified in the rhizosphere of *B. spiciformis* and 1025 ± 113 in the rhizosphere of *B. boehmii* ($t = -0.50$; $p = 0.43$; Table 2). The fire regime affected the number of OTUs ($t = 2.76$; $p = 0.03$), as well as the type of soil ($t = 2.06$; $p = 0.02$) because values were predominantly lower in ferric lixisol soils under low fire frequency (LFF) (Table 2). However, no significant differences were found in the interaction of soil \times plant species ($F = 33.21$; $p = 0.91$), fire \times plant species ($F = 15.32$; $p = 0.81$), or fire \times plant species ($F = 15.32$; $p = 0.81$).

Table 2. Mean and standard deviation number of operational taxonomic units (OTUs) and Shannon index values found in the rhizosphere of *Brachystegia spiciformis* and *Brachystegia boehmii* sampled in cambic arenosol and ferric lixisol soils under low (LFF) and high fire frequencies (HFF). Each value represents the mean \pm standard deviation ($n = 3$).

Soil Type	Species	Fire Regime	OTUs	Shannon Index
Cambic arenosol	<i>B. spiciformis</i>	HFF	1144 \pm 38	7.88 \pm 0.34
		LFF	1083 \pm 40	7.62 \pm 0.29
	<i>B. boehmii</i>	HFF	1076 \pm 224	7.87 \pm 0.27
		LFF	1086 \pm 82	7.53 \pm 0.45
Ferric lixisol	<i>B. spiciformis</i>	HFF	1072 \pm 150	7.71 \pm 0.57
		LFF	895 \pm 219	6.09 \pm 0.58
	<i>B. boehmii</i>	HFF	1083 \pm 160	7.44 \pm 0.64
		LFF	855 \pm 241	6.28 \pm 0.32

The bacterial- α -diversity expressed by the Shannon index was also lower in ferric lixisol soils under LFF in the rhizosphere of both *B. boehmii* and *B. spiciformis* (Table 2) without significant changes in microbial diversity between plant species ($t = -0.110$; $p = 0.985$). However, microbial diversity was affected by fire ($t = 2.111$; $p = 0.014$) and by the type of soil ($t = 2.331$; $p = 0.018$). The fire regime and type of soil also had a significant impact on bacterial β -diversity. A PCA plot based on Unifrac distances explained 63.46% of the observed variation (Supplementary Figure S2) and was able to separate the samples collected in ferric lixisol soils under LFF.

3.2. Composition of Soil Bacterial Communities

In total, the OTUs identified included 21 phyla, 51 classes, 98 orders, 193 families, 520 genera, and 1001 species. The most abundant phylum in all samples was *Actinobacteria* (35.52 \pm 0.08%), followed by *Proteobacteria* (17.41 \pm 0.03%), *Acidobacteria* (16.32 \pm 0.05%), *Firmicutes* (11.12 \pm 0.13%), and *Verrucomicrobia* (8.33 \pm 0.03%; Figure 1; Supplementary Table S2).

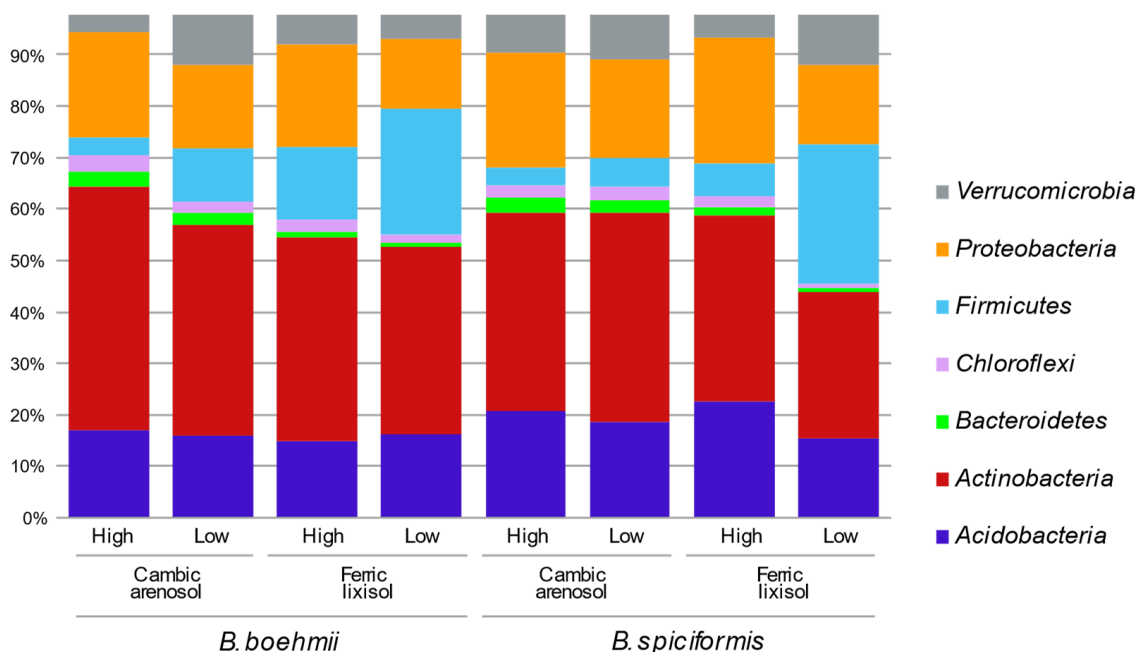


Figure 1. Relative abundance of bacterial phyla in the rhizosphere of *Brachystegia spiciformis* and *Brachystegia boehmii* sampled in cambic arenosol and ferric lixisol soils with low and high fire frequencies. Rare phyla, below 1% among all samples, or non-identified phyla were not included.

Differential abundance analysis revealed that *Verrucomicrobia* (LDA = 5.22; $p = 0.02$) was negatively impacted by HFF, while *Proteobacteria* (LDA = 5.35; $p = 0.01$), *Chloroflexi* (LDA = 4.63; $p = 0.02$), and *Dictyoglomi* (LDA = 3.87; $p = 0.01$) increased under HFF (Figure 1). In contrast, the type of soil affected the abundance of *Firmicutes* (LDA = 5.70; $p < 0.01$), which was higher in ferric lixisol soils under LFF, as well as *Bacteroidetes* (LDA = 4.74; $p < 0.01$), *Chloroflexi* (LDA = 4.63; $p = 0.04$), and *Nitrospirae* (LDA = 3.98; $p = 0.01$), which were all higher in cambic arenosol soils, independent of the fire regime.

Actinobacteria was the most frequent class across all samples (phylum *Actinobacteria*, $18.68 \pm 0.06\%$), followed by *Alphaproteobacteria* (phylum *Proteobacteria*, $12.30 \pm 0.03\%$) and *Bacilli* (phylum *Firmicutes*, $10.43 \pm 0.03\%$; Supplementary Table S3). We found no changes in the abundance of *Actinobacteria* or *Alphaproteobacteria* across plant species, fire regime, or soil type (always $p > 0.05$). However, the abundance of *Bacilli* was significantly affected by the type of soil ($F = 1.775$, $p = 0.022$) and fire regime ($F = 1.241$, $p = 0.027$), being especially prevalent in ferric lixisol soils under LFF ($23.73 \pm 8.43\%$ vs. 6.88 ± 1.22).

Four abundant genera were a core element of the microbiome, having similar abundances across plant species, type of soil, or fire regime (always $p > 0.05$): *Streptomyces* ($7.57 \pm 0.06\%$), *Gaiella* ($7.48 \pm 0.02\%$), *Chthoniobacter* ($6.63 \pm 0.03\%$), and *Bacillus* ($6.34 \pm 0.07\%$) (Supplementary Table S4).

Several bacterial genera, including *Blastochloris*, *Aciditerrimonas*, *Azoarcus*, *Blastocatella*, *Dactylosporangium*, *Actinophytocola*, and *Nordella*, were among the biomarkers detected in soils from HFF sites, while *Amycolatopsis* was more abundant in soils from LFF sites (Figure 2).

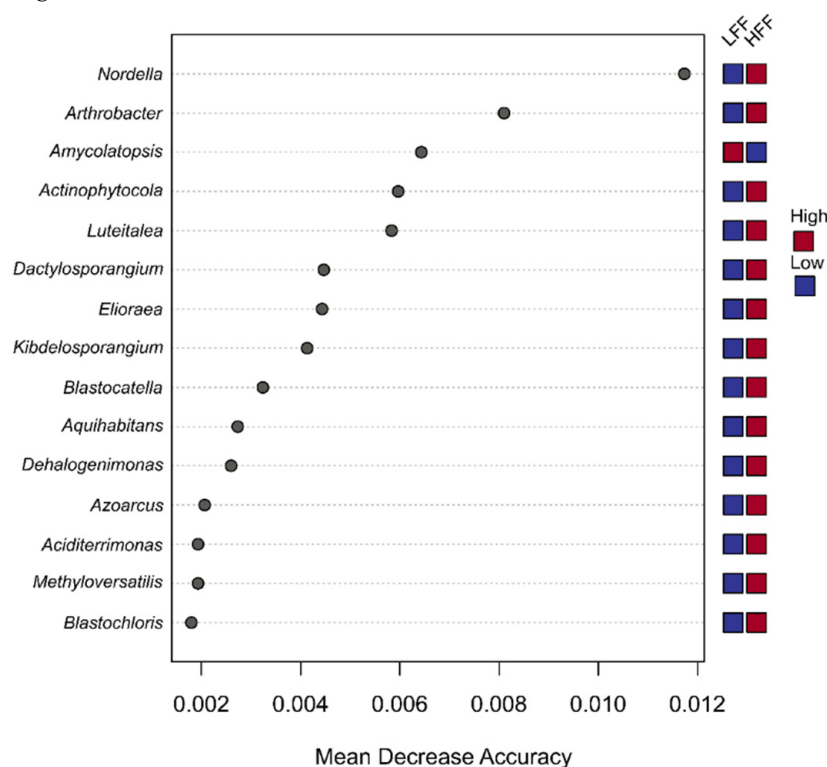


Figure 2. Genus taxonomic rank biomarkers detected in the high fire frequency and low fire frequency sites based on random forest analysis.

3.3. Co-Occurrence Patterns and Community Complexity

Two networks, representing microbial communities from sites with low and high fire frequencies, were constructed using a threshold value of 0.81. The HFF network comprised 162 nodes and 272 edges, while the LFF network comprised 177 nodes and 1091 edges. The networks were non-random and are unlikely to have occurred as a result of chance owing to the significant differences between the network parameters of the empirical networks and

their 100 corresponding random networks (Supplementary Table S5). The HFF network differed greatly from that of the low LFF network (Figure 3; Supplementary Table S5). The LFF network was larger with more nodes and edges, which increased the density of connections and thus the complexity of the overall network. In addition, the average network path distance was lower in the LFF network. We found smaller but slightly more numerous modules in the HFF network than in the LFF network, which was characterized by larger modules. Investigation of the contribution of different phylotypes to microbial community assembly revealed that only the diazotroph, *Ideonella*, was a keystone (module hub) genus in the HFF network, while *Dongia*, *Mesorhizobium*, and *Mycolicibacterium* were module hubs in the LFF network.

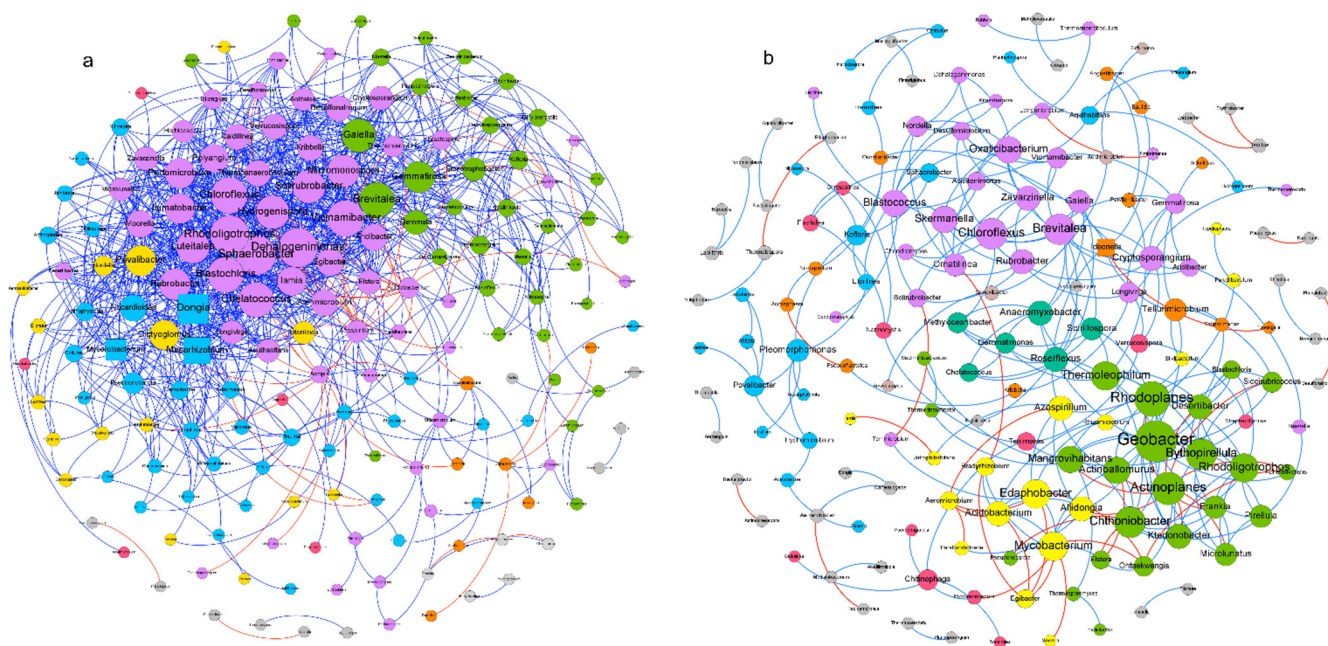


Figure 3. Empirical networks of bacterial communities in the low fire frequency (a) and high fire frequency (b) sites. The network nodes (bacterial genera) are colored according to modules (assemblage), while their sizes are proportional to their node degree. Peripheral nodes and connectors are round-shaped, while module hubs are square-shaped. The network edges represent significant direct interactions among phylotypes. The edges colored in red represent negative interactions, while those in blue are positive interactions.

3.4. Functional Analysis of Bacterial Communities

Among all samples, Tax4Fun identified 22 significant functional categories associated with amino acid transport and metabolism (16.5%), defense mechanisms (10.2%), replication recombination and repair (11.5%), energy production and conversion (12.3%), and inorganic ion transport and metabolism (8.25%), occupying more than 50% of the most dominant categories (Supplementary Figure S3). We did not detect significant changes in the functional categories between species, fire, or soil types, after adjustment for multiple testing ($p > 0.05$).

Additionally, PICRUSt2 identified 422 functional categories but with no specific clustering between samples (Supplementary Figure S4). The same pathways were found in *B. spiciformis*, and *B. boehmii* and no significant changes were detected between species, fire, or soil types, after adjustment for multiple testing ($p > 0.05$). The most important pathway found across all samples, PWY-3781 (Supplementary Table S6), was related to aerobic respiration I (cytochrome c).

3.5. Carbon and Nitrogen Isotopic Composition

The two *Brachystegia* species showed significantly different values of $\delta^{15}\text{N}$, as well as C/N ratios (Supplementary Table S7). The type of soil and fire intensity as well as interactions between them and species identity did not influence the values of $\delta^{13}\text{C}$, $\delta^{15}\text{N}$, or C/N ratio, although the fire frequency had close to a significant impact on $\delta^{15}\text{N}$. Overall, *B. spiciformis* had more enriched values of $\delta^{15}\text{N}$ when compared with *B. boehmii*, except in cambic arenosol soils exposed to HFF (Table 3). The isotopic analysis of *B. boehmii* revealed a value of $\delta^{15}\text{N}$ close to zero (0.7‰) in cambic arenosol soils under LFF.

Table 3. Values for $\delta^{15}\text{N}$ (‰), $\delta^{13}\text{C}$ (‰), N (%), C (%), and C/N ratio in *Brachystegia spiciformis* and *Brachystegia boehmii* leaves collected from plants grown in cambic arenosol and ferric lixisol soils, submitted to low (HFF) and high (LFF) fire frequency.

Soil Type	Species	Fire Regime	$\delta^{15}\text{N}$ (‰)	$\delta^{13}\text{C}$ (‰)	N (%)	C (%)	C/N
Cambic arenosol	<i>B. spiciformis</i>	HFF	1.8 ± 0.2	-28.2 ± 0.2	1.6 ± 0.2	43.9 ± 0.9	27.9 ± 2.3
		LFF	1.9 ± 0.2	-27.4 ± 0.3	1.8 ± 0.1	45.7 ± 0.8	26.1 ± 2.5
	<i>B. boehmii</i>	HFF	2.1 ± 0.1	-27.0 ± 0.3	1.5 ± 0.2	47.1 ± 1.1	31.1 ± 2.9
		LFF	0.7 ± 0.2	-28.2 ± 0.4	1.5 ± 0.2	47.5 ± 1.2	31.6 ± 3.0
Ferric lixisol	<i>B. spiciformis</i>	HFF	2.2 ± 0.2	-27.2 ± 0.2	1.7 ± 0.1	44.2 ± 1.4	26.9 ± 2.3
		LFF	2.0 ± 0.2	-27.8 ± 0.3	1.6 ± 0.1	44.8 ± 1.1	27.7 ± 2.5
	<i>B. boehmii</i>	HFF	1.6 ± 0.1	-27.6 ± 0.3	1.5 ± 0.2	48.0 ± 1.1	31.8 ± 2.9
		LFF	1.7 ± 0.2	-27.8 ± 0.4	1.3 ± 0.1	48.2 ± 0.2	36.7 ± 3.0

4. Discussion

4.1. Effects of Fire and Soil Types in Microbial Rhizosphere Diversity

As a traditional management practice, fire has historically shaped the structure, dynamics, and functionality of Miombo woodlands, creating a resilient ecosystem well adapted to disturbances [20]. However, the woodlands have recently undergone a rapid transformation due to anthropogenic activities, with impacts on the health, incomes, and livelihoods of billions of people [20]. The situation is bound to worsen with climate change and the intensification of the hydrological cycle. Understanding the dynamics of soil properties is thus fundamental to the sustainability of Miombo ecosystems and requires greater attention than it has received. To contribute to filling this gap, this study characterized the patterns of bacterial diversity in the soil under two pioneer Miombo species, *Brachystegia boehmii* and *Brachystegia spiciformis*, along a fire gradient in two soil types. The metagenomic approach used showed a high coverage in all of the samples (Supplementary Figure S1), suggesting that a considerable portion of the bacterial diversity was characterized in this study [48].

The rhizosphere of the two plant species shared a similar number of OTUs (1048 ± 107 in *B. spiciformis* and 1025 ± 113 in *B. boehmii*) that changed across fire regimes and the type of soil (Table 2). Bacterial diversity was within the range of values previously reported for the rhizosphere of *B. boehmii* (977–1391) in the Niassa Special Reserve (NSR), although no statistical differences were previously found between the type of soil or the fire regime [9]. Nevertheless, the bacterial diversity of *B. boehmii* and *B. spiciformis* was nearly two times higher than the values reported in the rhizosphere of *Colophospermum mopane* and *Combretum apiculatum*, ca. 4 [14], two legume trees from Mopane woodlands, the second most important ecoregion of Sub-Saharan Africa. Therefore, it is likely that the rhizobacteria of *B. spiciformis* and *B. boehmii* are fire-tolerant and/or can quickly recover under high fire frequency regimes [9,49]. In fact, the PCA plot of bacterial β -diversity (Supplementary Figure S2) was able to separate the samples collected in ferric lixisol soils under LFF, either as a direct result of heat or as an indirect effect of changes in soil properties [50]. Thus, although fire is often associated with the loss of bacterial diversity, our results suggest that the impact on bacterial diversity depends on species tolerance and the general environmental context [51]. Considering that fire is one of the main drivers of bio-

diversity in Miombo and that this ecosystem is exposed to frequent fires, Miombo species and their associated rhizobacteria have likely developed mechanisms of fire tolerance to grow quickly and occupy newly available niches in burned soils [9].

4.2. Disentangling Changes in the Rhizosphere Community Structure

In line with the results reported in other forest ecosystems (e.g., [52,53]), *Actinobacteria*, *Proteobacteria*, and *Acidobacteria* were the most abundant phyla (Figure 1). Bacteria belonging to these phyla usually participate in C, N, and S cycles and are also responsible for the production of secondary metabolites associated with plant resistance to pathogens [54]. Moreover, they are often adapted to extreme environmental conditions such as drought and high temperatures [55,56] and include symbiotic bacteria potentially relevant for plant nutrition and health [57–59]. However, the differential abundance analysis revealed that high-intensity fires affected negatively the abundance of *Verrucomicrobia*, while *Proteobacteria*, *Chloroflexi*, and *Dictyoglomi* increased under HFF (Figure 1). In contrast, the type of soil affected the abundance of *Firmicutes*, *Bacteroidetes*, *Chloroflexi*, and *Nitrospirae*, which were higher in cambic arenosol soils, independent of the fire regime (Figure 1; Supplementary Table S2). *Firmicutes*, *Bacteroidetes*, and *Chloroflexi* are considered sensitive biological indicators of agricultural soils as they integrate chitinolytic representatives with great ecological importance in the degradation of complex polysaccharides [60]. For instance, the abundance of Gram-positive *Firmicutes* or *Actinobacteria* phyla in the tomato rhizosphere is lower in diseased soils, enhancing the incidence of bacterial wilt disease [61]. Thus, despite the lower values of diversity found for ferric lixisol soils in the previous analyses, the high presence of *Firmicutes* in the rhizospheres of both plant species could indicate their role in healthy host-microbe relationships.

Several changes were also felt in the remaining taxonomical levels [62]. For instance, *Actinobacteria* was the most frequent class across all samples, followed by *Alphaproteobacteria* and *Bacilli* (Supplementary Table S3), all considered important chitinolytic bacteria [63]. These groups have been suggested to be central to biogeochemical cycling [64] and nitrogen fixation [65]. We found no changes in the abundance of *Actinobacteria* or *Alphaproteobacteria* across plant species, fire regime, or soil type, but the abundance of *Bacilli* was significantly higher in ferric lixisol soils under LFF. Endowed with a high genetic and metabolic diversity, *Bacilli* is usually spore forming, conferring stress tolerance to plants and functioning as plant-growth-promoting rhizobacteria [66].

Four abundant genera represented a core microbiome. They were found across samples without changes between plant species, type of soil, or fire regime: *Streptomyces*, *Gaiella*, *Chthoniobacter*, and *Bacillus* (Supplementary Table S4). *Streptomyces*, which were abundant in all the sites, regardless of soil type and fire frequency, are mycelium-forming bacteria with a central role in mineralization processes and production of secondary metabolites, including clinically useful antibiotics [67]. *Streptomyces* are also efficient root colonizers, linked to plant protection and growth [68]. Although the ecological role of *Gaiella* is poorly understood, phylogenetic studies point to thermo-, halo-, and radiotolerance [69], and its abundance in the rhizosphere of *B. boehmii* upon fire might be related to the thermo-tolerance of this species [9]. Additionally, its presence has been associated with events like denitrification, a potential source of nitrous oxide [70], metabolization of organic compounds, and nutrient cycling [71]. The genus *Chthoniobacter* has also been identified as one of the most abundant in the rhizosphere of *B. boehmii* [9]. The presence of bacteria responsible for carbohydrate metabolism may be important for stimulating the production of growth regulators, like auxin or ethylene, which enhance root growth [72]. Finally, *Bacillus* is a well-known plant-growth-promoting (PGP) genus that can survive in the soil for long periods under harsh environmental conditions. It has multiple ecological functions in the soil ecosystem that range from nutrient cycling to conferring stress tolerance and is one of the most commercially exploited bacteria in the agro-biotechnology industry [73].

Other bacterial genera, including *Blastochloris*, *Aciditerrimonas*, *Azoarcus*, *Blastocatella*, *Dactylosporangium*, *Actinophytocola*, and *Nordella*, were among the biomarkers detected

in soils from HFF sites, while *Amycolatopsis* was more abundant in soils from LFF sites (Figure 2). Apart from *Blastocatella*, which is a potential plant pathogen [74], most of the biomarkers detected in the HFF sites have been reported as beneficial to plants, contributing to nutrient cycling [75]. Thus, these bacterial genera might contribute to the ecological recovery of Miombo trees following frequent fires.

In fact, among all samples, predicted functional potential identified several categories involved in amino acid transport and metabolism, defense mechanisms, replication recombination and repair, energy production and conversion, inorganic ion transport, and metabolism, occupying more than 50% of the most dominant categories (Figure S3). This similarity between functional predictions despite taxonomic differences may be due to functional redundancy or the fact that mainly core “house-keeping” metabolisms were predicted. The most important pathway found across all samples, PWY-3781 (Supplementary Table S6), is related to aerobic respiration I (cytochrome c) and has been commonly reported in other soils, including those from Miombo [9]. Soil respiration plays an important role in global carbon cycling as well as in other nutrient cycles, such as nitrogen, and changes in the rate of respiration are an important indicator of climate change [76]. Although these results might reflect an intense bacterial activity, their eventual contribution to GHG emissions should be considered as it is a crucial element in the Miombo woodlands [77].

4.3. New Insights from Miombo Bacterial Ecological Networks

The construction of bacterial ecological networks can reveal information regarding community efficiency, complexity, and the role of keystone phylotypes [78]. The two networks found in this study were non-random and differ between fire regimes. The LFF network was larger, having more nodes and connections and a high complexity, while smaller but slightly more numerous modules were found in the HFF network (Figure 2). Less complex microbial networks are more susceptible to biotic and abiotic stress conditions and, most importantly, less complex communities are not as efficient at suppressing plant pathogens [79]. In addition, the average network path distance was lower in the LFF network. This suggests that the bacterial communities in the LFF network had a higher potential for mutualist interactions and transmission of chemical signals among phylotypes than in the HFF network. Network modularity is an important topological feature for the assessment of community resilience and stability. We found smaller but slightly more numerous modules in the HFF network than in the LFF network, which was characterized by larger modules. From an ecological perspective, more small modules can increase community resilience if they all perform their ecological functions simultaneously [80]. Therefore, higher modularity in the HFF network may be a response to increased fire frequency.

Our results also indicate that only the diazotroph, *Ideonella*, was a keystone (module hub) genus in the HFF network, while *Dongia*, *Mesorhizobium*, and *Mycolicibacterium* were module hubs in the LFF network. *Mesorhizobium* is an important plant-growth-promoting bacteria that contributes to root nodulation [81], while *Mycolicibacterium* has been reported to support plant growth by enhancing plant–microbe symbiosis, and contributing to plant development, phytopathogen suppression, and tolerance to biotic and abiotic stresses [82]. These features could explain why these phylotypes had the strongest contributions to bacterial community co-occurrence patterns.

The predominance of *Dongia*, *Mesorhizobium*, and *Mycolicibacterium* module hubs in the LFF network suggest differences in symbiotic associations found between soils and fire regimes, but not between the two *Brachystegia* species (Table 3). The isotopic analysis of *B. boehmii* revealed a value of $\delta^{15}\text{N}$ close to zero (0.7‰) in cambic arenosol soils under LFF, which suggests symbiosis with N-fixing bacteria in this legume species. The ability of legumes to thrive in low fertility soils and to compete successfully with other plants is attributed, partially, to the symbiotic associations that give them the capacity to fix atmospheric nitrogen. However, symbiotic bacterial species have only been identified for a small proportion of legumes [83]. Additionally, taking into account that the reported values corresponding to N_2 -fixing species are usually <0 [18], any conclusion in this regard

cannot be drawn without clear proof of concept analysis. Root inputs to the soil often generate nutritionally distinct microenvironments that shape differences in the microbial activity in the rhizosphere of plants [84]. However, how generalizable these results are across plant species and soils is still under debate, especially when considering poorly studied soils such as those of African dry woodlands. These questions are important to infer ecosystem functioning as the ratio of carbon to nitrogen fixation has a direct impact on litter decomposition and nitrogen cycling, for which we recommend future functional studies.

5. Conclusions

In this study, a comparative analysis of the rhizospheres of two typical Miombo species, *B. spiciformis* and *B. boehmii*, was performed. The metagenomic data reported here have the potential to improve our understanding of the overall microbial community diversity and the potential functions of the microbial community. We showed that, independently of the environmental conditions, the dynamics of bacterial diversity in the rhizosphere of *B. spiciformis* and *B. boehmii* was considerably high and multifunctional, with strong potentialities to produce bioactive compounds as well as nutrient mobilization. Therefore, this study provides the opportunity to guide the future isolation and cultivation of microbes of interest and the functional validation of microbial genes and pathways.

Supplementary Materials: The following supporting information can be downloaded at <https://www.mdpi.com/article/10.3390/f13111840/s1>, Figure S1: Rarefaction curves of rhizobacteria from *B. spiciformis* (blue) and *B. boehmii* (red). Figure S2: Principal coordinates analysis of the weighted UniFrac distance matrix. Each point corresponds to a sample and indicates the effect of fire, soil, and species: circles: *B. spiciformis*; *B. boehmii*: squares. LFF in ferric lixisol soils: yellow. HFF in ferric lixisol soils: red. LFF in cambic arenosol soils: light blue. HFF in cambic arenosol soils: dark blue. Figure S3: Functional categories predicted by Tax4Fun in the rhizosphere of *B. spiciformis* and *B. boehmii*. Figure S4: Scatter plot showing the correlation between the functional profiles across samples of the two groups of species, *Brachystegia spiciformis* (red) and *Brachystegia boehmii* (blue). Table S1: Statistics of raw data of Miombo soil samples collected from the rhizosphere of *Brachystegia spiciformis* (SBSP) and *Brachystegia boehmii* (SBBP). Table S2: ANOVA results showing bacterial differences at the phylum level between the two plant species, the type of soil type, and the fire frequency (SS: sum of squares; df: degrees of freedom). Significant values are indicated in bold. Table S3: Relative abundance of bacterial classes in the rhizosphere of *Brachystegia spiciformis* and *Brachystegia boehmii* sampled in cambic arenosol and ferric lixisol soils with low and high fire frequencies. Table S4: Relative abundance of the most frequent bacterial genus (>1% across all samples) in the rhizosphere of *Brachystegia spiciformis* and *Brachystegia boehmii* sampled in cambic arenosol and ferric lixisol soils with low and high fire frequencies. Table S5: Topological properties of the empirical networks and their 100 corresponding random networks. Table S6: Top pathways detected by Picrust in samples. Table S7: Two-way ANOVA of effects of species, soil type, and fire frequency on $\delta^{13}\text{C}$, $\delta^{15}\text{N}$, and CN ratio. SS: sum of squares; df: degrees of freedom.

Author Contributions: Conceptualization A.I.R.-B., N.S.R. and T.M.; methodology, A.I.R.-B., N.S.R., J.C.R. and T.M.; formal analysis, C.B.S.A., C.O., I.S.A.M., A.I.R.-B., J.J., C.M., N.S.R. and T.M.; investigation, C.B.S.A., C.O., I.S.A.M., A.I.R.-B., J.J., C.M., N.S.R., J.C.R. and T.M.; data curation, C.B.S.A., C.O., I.S.A.M., A.I.R.-B., J.J., C.M., N.S.R. and T.M.; writing—original draft preparation, C.B.S.A., C.O., I.M. and A.I.R.-B.; visualization, C.O., C.B.S.A., I.S.A.M., I.M. and C.O.; supervision, A.I.R.-B. and C.M.; project administration, A.I.R.-B.; funding acquisition, A.I.R.-B. All authors have read and agreed to the published version of the manuscript.

Funding: This research received national funds through Camões, Instituto da Cooperação e da Língua and the FCT—Fundação para a Ciência e a Tecnologia, I.P., Portugal through the research units UIDB/00239/2020 (CEF), UIDP/00329/2020 (cE3c), the grant SFRH/BD/113951/2015, and under the Scientific Employment Stimulus-Individual Call (CEEC Individual)-2021.01107.CEECIND/CP1689/CT0001 (IM) and Howard Hughes Medical Institute: Grant Number 54108287.

Institutional Review Board Statement: Not applicable.

Informed Consent Statement: Not applicable.

Data Availability Statement: The datasets generated during and/or analyzed during the current study are available at 10.5281/zenodo.7194179.

Acknowledgments: We thank the excellent staff of Gorongosa National Park; Marc Stahlmans for the critical review of this paper; as well as Jason Denlinger, Berta Cuambe, and Matt Jordans for their support of this work.

Conflicts of Interest: The authors declare no conflict of interest. The funders had no role in the design of the study; in the collection, analyses, or interpretation of data; in the writing of the manuscript; or in the decision to publish the results.

References

1. WWF Miombo Eco-Region. “Home of the Zambezi”. *Conservation Strategy: 2011–2020*; WWF: Harare, Zimbabwe, 2012.
2. Macave, O.A.; Ribeiro, N.S.; Ribeiro, A.I.; Chauque, A.; Bandeira, R.; Branquinho, C.; Washington-Allen, R. Modelling Above-ground Biomass of Miombo Woodlands in Niassa Special Reserve, Northern Mozambique. *Forests* **2022**, *13*, 311. [[CrossRef](#)]
3. Jew, E.K.K.; Dougill, A.J.; Sallu, S.M.; O’Connell, J.; Benton, T.G. Miombo woodland under threat: Consequences for tree diversity and carbon storage. *For. Ecol. Manag.* **2016**, *361*, 144–153. [[CrossRef](#)]
4. Lupala, Z.J.; Lusambo, L.P.; Ngaga, Y.M. Management, Growth, and Carbon Storage in Miombo Woodlands of Tanzania. *Int. J. For. Res.* **2014**, *2014*, 629317. [[CrossRef](#)]
5. Ribeiro-Barros, A.I.; Silva, M.J.; Moura, I.; Ramalho, J.C.; Máguas-Hanson, C.; Ribeiro, N.S. The Potential of Tree and Shrub Legumes in Agroforestry Systems. In *Nitrogen in Agriculture-Updates*; IntechOpen: London, UK, 2018; ISBN 978-953-51-3769-6.
6. Ribeiro, N.S.; Saatchi, S.S.; Shugart, H.H.; Washington-Allen, R.A. Aboveground biomass and leaf area index (LAI) mapping for Niassa Reserve, northern Mozambique. *J. Geophys. Res. Biogeosciences* **2008**, *113*. [[CrossRef](#)]
7. Chinder, G.B.; Hattas, D.; Massad, T.J. Growth and functional traits of *Julbernardia globiflora* (Benth) resprouts and seedlings in response to fire frequency and herbivory in miombo woodlands. *S. Afr. J. Bot.* **2020**, *135*, 476–483. [[CrossRef](#)]
8. Ribeiro, N.S.; Armstrong, A.H.; Fischer, R.; Kim, Y.S.; Shugart, H.H.; Ribeiro-Barros, A.I.; Chauque, A.; Tear, T.; Washington-Allen, R.; Bandeira, R.R. Prediction of forest parameters and carbon accounting under different fire regimes in Miombo woodlands, Niassa Special Reserve, Northern Mozambique. *For. Policy Econ.* **2021**, *133*, 102625. [[CrossRef](#)]
9. Maquia, I.S.A.; Fareleira, P.; Castro, I.V.E.; Soares, R.; Brito, D.R.A.; Mbanze, A.A.; Chauque, A.; Máguas, C.; Ezeokoli, O.T.; Ribeiro, N.S.; et al. The nexus between fire and soil bacterial diversity in the african miombo woodlands of niassa special reserve, mozambique. *Microorganisms* **2021**, *9*, 1562. [[CrossRef](#)]
10. Cardenas, E.; Kranabetter, J.M.; Hope, G.; Maas, K.R.; Hallam, S.; Mohn, W.W. Forest harvesting reduces the soil metagenomic potential for biomass decomposition. *ISME J.* **2015**, *9*, 2465–2476. [[CrossRef](#)]
11. Ahemad, M.; Kibret, M. Mechanisms and applications of plant growth promoting rhizobacteria: Current perspective. *J. King Saud Univ.-Sci.* **2014**, *26*, 1–20. [[CrossRef](#)]
12. de Souza, L.C.; Procópio, L. The profile of the soil microbiota in the Cerrado is influenced by land use. *Appl. Microbiol. Biotechnol.* **2021**, *105*, 4791–4803. [[CrossRef](#)]
13. Neary, D.G.; Klopatek, C.C.; DeBano, L.F.; Ffolliott, P.F. Fire effects on belowground sustainability: A review and synthesis. In *Forest Ecology and Management*; Elsevier: Amsterdam, The Netherlands, 1999; Volume 122, pp. 51–71.
14. Maquia, I.S.; Fareleira, P.; Castro, I.V.E.; Brito, D.R.A.; Soares, R.; Chauque, A.; Ferreira-Pinto, M.M.; Lumini, E.; Berruti, A.; Ribeiro, N.S.; et al. Mining the microbiome of key species from african savanna woodlands: Potential for soil health improvement and plant growth promotion. *Microorganisms* **2020**, *8*, 1291. [[CrossRef](#)] [[PubMed](#)]
15. Teixeira, H.; Rodríguez-Echeverría, S. Identification of symbiotic nitrogen-fixing bacteria from three African leguminous trees in Gorongosa National Park. *Syst. Appl. Microbiol.* **2016**, *39*, 350–358. [[CrossRef](#)] [[PubMed](#)]
16. Kurdali, F.; Al-Shamma’a, M. Natural abundances of ^{15}N and ^{13}C in leaves of some N_2 -fixing and non- N_2 -fixing trees and shrubs in Syria. *Isotopes Environ. Health Stud.* **2009**, *45*, 198–207. [[CrossRef](#)] [[PubMed](#)]
17. Craine, J.M.; Brookshire, E.N.J.; Cramer, M.D.; Hasselquist, N.J.; Koba, K.; Marin-Spiotta, E.; Wang, L.; Craine, J.M.; Ventures, J.; Cramer, M.D.; et al. Ecological interpretations of nitrogen isotope ratios of terrestrial plants and soils. *Plant Soil* **2015**, *396*, 1–26. [[CrossRef](#)]
18. Ulm, F.; Hellmann, C.; Cruz, C.; Máguas, C. N/P imbalance as a key driver for the invasion of oligotrophic dune systems by a woody legume. *Oikos* **2017**, *126*, gc735. [[CrossRef](#)]
19. del Amor, F.M.; Cuadra-Crespo, P. Alleviation of salinity stress in broccoli using foliar urea or methyl-jasmonate: Analysis of growth, gas exchange, and isotope composition. *Plant Growth Regul.* **2011**, *63*, 55–62. [[CrossRef](#)]
20. Ribeiro, N.S.; Grundy, I.M.; Gonçalves, F.M.P.; Moura, I.; Santos, M.J.; Kamoto, J.; Ribeiro-Barros, A.I.; Gandiwa, E. People in the Miombo Woodlands: Socio-Ecological Dynamics. In *Miombo Woodlands in a Changing Environment: Securing the Resilience and Sustainability of People and Woodlands*; Springer International Publishing: Manhattan, NY, USA, 2020; pp. 55–100.
21. Kotteck, M.; Grieser, J.; Beck, C.; Rudolf, B.; Rubel, F. World map of the Köppen-Geiger climate classification updated. *Meteorol. Z.* **2006**, *15*, 259–263. [[CrossRef](#)]
22. Campbell, B.M. *The Miombo in Transition: Woodlands and Welfare in Africa*; Center for International Forestry Research: Bogor Barat, Indonesia, 1996; ISBN 9798764072.

23. Ryan, C.M.; Williams, M. How does fire intensity and frequency affect miombo woodland tree populations and biomass? *Ecol. Appl.* **2011**, *21*, 48–60. [[CrossRef](#)]
24. Fernandes, J.F. Os solos do Parque Nacional da Gorongosa. *Inst. Investig. Agronómica Moçambique Commun.* **1968**, *19*, 1–78.
25. Caporaso, J.G.; Kuczynski, J.; Stombaugh, J.; Bittinger, K.; Bushman, F.D.; Costello, E.K.; Fierer, N.; Peña, A.G.; Goodrich, J.K.; Gordon, J.I.; et al. QIIME allows analysis of high-throughput community sequencing data. *Nat. Methods* **2010**, *7*, 335–336. [[CrossRef](#)]
26. Magoč, T.; Salzberg, S.L. FLASH: Fast length adjustment of short reads to improve genome assemblies. *Bioinformatics* **2011**, *27*, 2957–2963. [[CrossRef](#)] [[PubMed](#)]
27. Edgar, R.C.; Haas, B.J.; Clemente, J.C.; Quince, C.; Knight, R. UCHIME improves sensitivity and speed of chimera detection. *Bioinformatics* **2011**, *27*, 2194–2200. [[CrossRef](#)]
28. Rognes, T.; Flouri, T.; Nichols, B.; Quince, C.; Mahé, F. VSEARCH: A versatile open source tool for metagenomics. *PeerJ* **2016**, *2016*, e2584. [[CrossRef](#)] [[PubMed](#)]
29. Greengenes. Available online: <https://greengenes.lbl.gov/Download/> (accessed on 12 October 2022).
30. Alpha_Diversity.Py—Calculate Alpha Diversity on Each Sample in an Otu Table, Using a Variety of Alpha Diversity Metrics—Homepage. Available online: http://qiime.org/scripts/alpha_diversity.html (accessed on 12 October 2022).
31. Lozupone, C.; Knight, R. UniFrac: A new phylogenetic method for comparing microbial communities. *Appl. Environ. Microbiol.* **2005**, *71*, 8228–8235. [[CrossRef](#)] [[PubMed](#)]
32. Segata, N.; Izard, J.; Waldron, L.; Gevers, D.; Miropolsky, L.; Garrett, W.S.; Huttenhower, C. Metagenomic biomarker discovery and explanation. *Genome Biol.* **2011**, *12*, R60. [[CrossRef](#)] [[PubMed](#)]
33. Breiman, L. Random forests. *Mach. Learn.* **2001**, *45*, 5–32. [[CrossRef](#)]
34. Deng, Y.; Jiang, Y.H.; Yang, Y.; He, Z.; Luo, F.; Zhou, J. Molecular ecological network analyses. *BMC Bioinform.* **2012**, *13*, 113. [[CrossRef](#)]
35. Maslov, S.; Sneppen, K. Specificity and stability in topology of protein networks. *Science* **2002**, *296*, 910–913. [[CrossRef](#)]
36. Guimerà, R.; Amaral, L.A.N. Functional cartography of complex metabolic networks. *Nature* **2005**, *433*, 895–900. [[CrossRef](#)]
37. Aßhauer, K.P.; Wemheuer, B.; Daniel, R.; Meinicke, P. Tax4Fun: Predicting functional profiles from metagenomic 16S rRNA data. *Bioinformatics* **2015**, *31*, 2882–2884. [[CrossRef](#)]
38. Chong, J.; Liu, P.; Zhou, G.; Xia, J. Using MicrobiomeAnalyst for comprehensive statistical, functional, and meta-analysis of microbiome data. *Nat. Protoc.* **2020**, *15*, 799–821. [[CrossRef](#)] [[PubMed](#)]
39. Douglas, G.M.; Maffei, V.J.; Zaneveld, J.; Yurgel, S.N.; Brown, J.R.; Taylor, C.M.; Huttenhower, C.; Langille, M.G.I. PICRUSt2: An improved and extensible approach for metagenome inference. *bioRxiv* **2019**, 672295. [[CrossRef](#)]
40. Louca, S.; Doebeli, M. Efficient comparative phylogenetics on large trees. *Bioinformatics* **2018**, *34*, 1053–1055. [[CrossRef](#)] [[PubMed](#)]
41. Ye, Y.; Doak, T.G. A parsimony approach to biological pathway reconstruction/inference for genomes and metagenomes. *PLoS Comput. Biol.* **2009**, *5*, e1000465. [[CrossRef](#)] [[PubMed](#)]
42. Caspi, R.; Billington, R.; Fulcher, C.A.; Keseler, I.M.; Kothari, A.; Krummenacker, M.; Latendresse, M.; Midford, P.E.; Ong, Q.; Ong, W.K.; et al. The MetaCyc database of metabolic pathways and enzymes. *Nucleic Acids Res.* **2018**, *46*, D633–D639. [[CrossRef](#)]
43. Parks, D.H.; Tyson, G.W.; Hugenholtz, P.; Beiko, R.G. STAMP: Statistical analysis of taxonomic and functional profiles. *Bioinformatics* **2014**, *30*, 3123–3124. [[CrossRef](#)]
44. Benjamini, Y.; Hochberg, Y. Controlling the False Discovery Rate: A Practical and Powerful Approach to Multiple Testing. *J. R. Stat. Soc. Ser. B* **1995**, *57*, 289–300. [[CrossRef](#)]
45. Duro, N.; Batista-Santos, P.; da Costa, M.; Maia, R.; Castro, I.V.; Ramos, M.; Ramalho, J.C.; Pawlowski, K.; Máguas, C.; Ribeiro-Barros, A. The impact of salinity on the symbiosis between *Casuarina glauca* Sieb. ex Spreng. and N₂-fixing *Frankia* bacteria based on the analysis of Nitrogen and Carbon metabolism. *Plant Soil* **2016**, *398*, 327–337. [[CrossRef](#)]
46. Sampaio, L.; Freitas, R.; Máguas, C.; Rodrigues, A.; Quintino, V. Coastal sediments under the influence of multiple organic enrichment sources: An evaluation using carbon and nitrogen stable isotopes. *Mar. Pollut. Bull.* **2010**, *60*, 272–282. [[CrossRef](#)]
47. Coleman, M.; Meier-Augenstein, W. Ignoring IUPAC guidelines for measurement and reporting of stable isotope abundance values affects us all. *Rapid Commun. Mass Spectrom.* **2014**, *28*, 1953–1955. [[CrossRef](#)]
48. Zhou, L.; Ng, H.K.; Drautz-Moses, D.I.; Schuster, S.C.; Beck, S.; Kim, C.; Chambers, J.C.; Loh, M. Systematic evaluation of library preparation methods and sequencing platforms for high-throughput whole genome bisulfite sequencing. *Sci. Rep.* **2019**, *9*, 10383. [[CrossRef](#)] [[PubMed](#)]
49. Kara, O.; Bolat, I. Short-term effects of wildfire on microbial biomass and abundance in black pine plantation soils in Turkey. *Ecol. Indic.* **2009**, *9*, 1151–1155. [[CrossRef](#)]
50. Docherty, K.M.; Balsler, T.C.; Bohannon, B.J.M.; Gutknecht, J.L.M. Soil microbial responses to fire and interacting global change factors in a California annual grassland. *Biogeochemistry* **2012**, *109*, 63–83. [[CrossRef](#)]
51. Whitman, T.; Whitman, E.; Woolet, J.; Flannigan, M.D.; Thompson, D.K.; Parisien, M.A. Soil bacterial and fungal response to wildfires in the Canadian boreal forest across a burn severity gradient. *Soil Biol. Biochem.* **2019**, *138*, 107571. [[CrossRef](#)]
52. Fernández-González, A.J.; Martínez-Hidalgo, P.; Cobo-Díaz, J.F.; Villadas, P.J.; Martínez-Molina, E.; Toro, N.; Tringe, S.G.; Fernández-López, M. The rhizosphere microbiome of burned holm-oak: Potential role of the genus *Arthrobacter* in the recovery of burned soils. *Sci. Rep.* **2017**, *7*, 6008. [[CrossRef](#)]

53. Villadas, P.J.; Díaz-Díaz, S.; Rodríguez-Rodríguez, A.; del Arco-Aguilar, M.; Fernández-González, A.J.; Pérez-Yépez, J.; Arbelo, C.; González-Mancebo, J.M.; Fernández-López, M.; León-Barrios, M. The soil microbiome of the laurel forest in garajonay national park (La Gomera, Canary Islands): Comparing unburned and burned habitats after a wildfire. *Forests* **2019**, *10*, 1051. [[CrossRef](#)]
54. Castañeda, L.E.; Barbosa, O. Metagenomic analysis exploring taxonomic and functional diversity of soil microbial communities in Chilean vineyards and surrounding native forests. *PeerJ* **2017**, *2017*, e3098. [[CrossRef](#)] [[PubMed](#)]
55. de Araujo, A.S.F.; Mendes, L.W.; Lemos, L.N.; Antunes, J.E.L.; Beserra, J.E.A.; de Lyra, M.D.C.C.P.; Figueiredo, M.D.V.B.; Lopes, C.D.A.; Gomes, R.L.F.; Bezerra, W.M.; et al. Protist species richness and soil microbiome complexity increase towards climax vegetation in the Brazilian Cerrado. *Commun. Biol.* **2018**, *1*, 135. [[CrossRef](#)]
56. de Souza, L.C.; Procópio, L. The adaptations of the microbial communities of the savanna soil over a period of wildfire, after the first rains, and during the rainy season. *Environ. Sci. Pollut. Res.* **2022**, *29*, 14070–14082. [[CrossRef](#)]
57. Ganz, H.H.; Karaoz, U.; Getz, W.M.; Versfeld, W.; Brodie, E.L. Diversity and structure of soil bacterial communities associated with vultures in an African savanna. *Ecosphere* **2012**, *3*, art47. [[CrossRef](#)]
58. Lan, G.; Li, Y.; Jatoi, M.T.; Tan, Z.; Wu, Z.; Xie, G. Change in Soil Microbial Community Compositions and Diversity Following the Conversion of Tropical Forest to Rubber Plantations in Xishuangbanna, Southwest China. *Trop. Conserv. Sci.* **2017**, *10*, 1–14. [[CrossRef](#)]
59. Dube, J.P.; Valverde, A.; Steyn, J.M.; Cowan, D.A.; van der Waals, J.E. Differences in bacterial diversity, Composition and function due to long-term agriculture in soils in the Eastern Free State of South Africa. *Diversity* **2019**, *11*, 61. [[CrossRef](#)]
60. Li, Y.P.; You, L.X.; Yang, X.J.; Yu, Y.S.; Zhang, H.T.; Yang, B.; Chorover, J.; Feng, R.W.; Rensing, C. Extrapolymeric substances (EPS) in *Mucilaginibacter rubeus* P2 displayed efficient metal(loid) bio-adsorption and production was induced by copper and zinc. *Chemosphere* **2022**, *291*, 132712. [[CrossRef](#)] [[PubMed](#)]
61. Lee, S.M.; Kong, H.G.; Song, G.C.; Ryu, C.M. Disruption of Firmicutes and Actinobacteria abundance in tomato rhizosphere causes the incidence of bacterial wilt disease. *ISME J.* **2021**, *15*, 330–347. [[CrossRef](#)]
62. Philippot, L.; Andersson, S.G.E.; Battin, T.J.; Prosser, J.I.; Schimel, J.P.; Whitman, W.B.; Hallin, S. The ecological coherence of high bacterial taxonomic ranks. *Nat. Rev. Microbiol.* **2010**, *8*, 523–529. [[CrossRef](#)]
63. Beier, S.; Bertilsson, S. Bacterial chitin degradation-mechanisms and ecophysiological strategies. *Front. Microbiol.* **2013**, *4*, 149. [[CrossRef](#)]
64. Pointing, S.B.; Chan, Y.; Lacap, D.C.; Lau, M.C.Y.; Jurgens, J.A.; Farrell, R.L. Highly specialized microbial diversity in hyper-arid polar desert. *Proc. Natl. Acad. Sci. USA* **2009**, *106*, 19964–19969. [[CrossRef](#)]
65. Black, M.; Moolhuijzen, P.; Chapman, B.; Barrero, R.; Howieson, J.; Hungria, M.; Bellgard, M. The genetics of symbiotic nitrogen fixation: Comparative genomics of 14 rhizobia strains by resolution of protein clusters. *Genes* **2012**, *3*, 138–166. [[CrossRef](#)]
66. Fan, B.; Wang, C.; Song, X.; Ding, X.; Wu, L.; Wu, H.; Gao, X.; Borriss, R. Corrigendum: *Bacillus velezensis* FZB42 in 2018: The gram-positive model strain for plant growth promotion and biocontrol. *Front. Microbiol.* **2018**, *9*, 2491, Erratum in: *Front. Microbiol.* **2019**, *10*, 1279. [[CrossRef](#)]
67. Osama, N.; Bakeer, W.; Raslan, M.; Soliman, H.A.; Abdelmohsen, U.R.; Sebak, M. Anti-cancer and antimicrobial potential of five soil Streptomycetes: A metabolomics-based study. *R. Soc. Open Sci.* **2022**, *9*, 211509. [[CrossRef](#)]
68. Vergnes, S.; Gayraud, D.; Veysseyre, M.; Toulotte, J.; Martinez, Y.; Dumont, V.; Bouchez, O.; Rey, T.; Dumas, B. Phyllosphere colonization by a soil *Streptomyces* sp. promotes plant defense responses against fungal infection. *Mol. Plant-Microbe Interact.* **2020**, *33*, 223–234. [[CrossRef](#)] [[PubMed](#)]
69. Severino, R.; Froufe, H.J.C.; Barroso, C.; Albuquerque, L.; Lobo-da-Cunha, A.; da Costa, M.S.; Egas, C. High-quality draft genome sequence of *Gaiella occulta* isolated from a 150 meter deep mineral water borehole and comparison with the genome sequences of other deep-branching lineages of the phylum Actinobacteria. *Microbiologyopen* **2019**, *8*, e00840. [[CrossRef](#)]
70. Parente, C.E.T.; Brito, E.M.S.; Caretta, C.A.; Cervantes-Rodríguez, E.A.; Fábila-Canto, A.P.; Vollú, R.E.; Seldin, L.; Malm, O. Bacterial diversity changes in agricultural soils influenced by poultry litter fertilization. *Braz. J. Microbiol.* **2021**, *52*, 675–686. [[CrossRef](#)] [[PubMed](#)]
71. Pertile, M.; Sousa, R.M.S.; Mendes, L.W.; Antunes, J.E.L.; Oliveira, L.M.D.S.; de Araujo, F.F.; Melo, V.M.M.; Araujo, A.S.F. Response of soil bacterial communities to the application of the herbicides imazethapyr and flumyazin. *Eur. J. Soil Biol.* **2021**, *102*, 103252. [[CrossRef](#)]
72. Corrêa, L.D.R.; Paim, D.C.; Schwambach, J.; Fett-Neto, A.G. Carbohydrates as regulatory factors on the rooting of *Eucalyptus saligna* Smith and *Eucalyptus globulus* Labill. *Plant Growth Regul.* **2005**, *45*, 63–73. [[CrossRef](#)]
73. Radhakrishnan, R.; Hashem, A.; Abd Allah, E.F. *Bacillus*: A biological tool for crop improvement through bio-molecular changes in adverse environments. *Front. Physiol.* **2017**, *8*, 667. [[CrossRef](#)] [[PubMed](#)]
74. Joshi, S.; Jaggi, V.; Gangola, S.; Singh, A.; Sah, V.K.; Sahgal, M. Contrasting rhizosphere bacterial communities of healthy and wilted *Dalbergia sissoo* Roxb. *forests. Rhizosphere* **2021**, *17*, 100295. [[CrossRef](#)]
75. Meier, M.A.; Lopez-Guerrero, M.G.; Guo, M.; Schmer, M.R.; Herr, J.R.; Schnable, J.C.; Alfano, J.R.; Yang, J. Rhizosphere Microbiomes in a Historical Maize-Soybean Rotation System Respond to Host Species and Nitrogen Fertilization at the Genus and Subgenus Levels. *Appl. Environ. Microbiol.* **2021**, *87*, e0313220. [[CrossRef](#)]
76. Moe, L.A. Amino acids in the rhizosphere: From plants to microbes. *Am. J. Bot.* **2013**, *100*, 1692–1705. [[CrossRef](#)]
77. Ribeiro, N.S.; Cangela, A.; Chauque, A.; Bandeira, R.R.; Ribeiro-Barros, A.I. Characterisation of spatial and temporal distribution of the fire regime in Niassa National Reserve, northern Mozambique. *Int. J. Wildl. Fire* **2017**, *26*, 1021–1029. [[CrossRef](#)]

78. Ezeokoli, O.T.; Nuaila, V.N.A.; Obieze, C.C.; Muetanene, B.A.; Fraga, I.; Tesinde, M.N.; Ndayiragije, A.; Coutinho, J.; Melo, A.M.P.; Adeleke, R.A.; et al. Assessing the impact of rice cultivation and off-season period on dynamics of soil enzyme activities and bacterial communities in two agro-ecological regions of mozambique. *Agronomy* **2021**, *11*, 694. [[CrossRef](#)]
79. Santolini, M.; Barabási, A.L. Predicting perturbation patterns from the topology of biological networks. *Proc. Natl. Acad. Sci. USA* **2018**, *115*, E6375–E6383. [[CrossRef](#)] [[PubMed](#)]
80. Zhang, B.; Ning, D.; Yang, Y.; Van Nostrand, J.D.; Zhou, J.; Wen, X. Biodegradability of wastewater determines microbial assembly mechanisms in full-scale wastewater treatment plants. *Water Res.* **2020**, *169*, 115276. [[CrossRef](#)] [[PubMed](#)]
81. Pandey, R.P.; Srivastava, A.K.; Gupta, V.K.; O'Donovan, A.; Ramteke, P.W. Enhanced yield of diverse varieties of chickpea (*Cicer arietinum* L.) by different isolates of *Mesorhizobium ciceri*. *Environ. Sustain.* **2018**, *1*, 425–435. [[CrossRef](#)]
82. del Barrio-Duque, A.; Ley, J.; Samad, A.; Antonielli, L.; Sessitsch, A.; Compant, S. Beneficial Endophytic Bacteria-Serendipita indica Interaction for Crop Enhancement and Resistance to Phytopathogens. *Front. Microbiol.* **2019**, *10*, 2888. [[CrossRef](#)] [[PubMed](#)]
83. Weir, B.S.; Turner, S.J.; Silvester, W.B.; Park, D.C.; Young, J.M. Unexpectedly diverse *Mesorhizobium* strains and *Rhizobium leguminosarum* nodulate native legume genera of New Zealand, while introduced legume weeds are nodulated by *Bradyrhizobium* species. *Appl. Environ. Microbiol.* **2004**, *70*, 5980–5987. [[CrossRef](#)] [[PubMed](#)]
84. Wang, G.; Li, J.; Liu, X.; Li, X. Variations in carbon isotope ratios of plants across a temperature gradient along the 400 mm isoline of mean annual precipitation in north China and their relevance to paleovegetation reconstruction. *Quat. Sci. Rev.* **2013**, *63*, 83–90. [[CrossRef](#)]